Influence of Cr_2AlC on the thermal shock and corrosion resistance of low carbon Al_2O_3-C refractory

Zihao Wu, Junfeng Chen*, Wen Yan, Nan Li
Wuhan University of Science and Technology
Wuhan, China
*E-mail: chenjunfengref@wust.edu.cn

1 Background

2 Experiment

3 Results

4 Conclusions

1. Background

Steel products are now widely used in various fields, and steel metallurgy technology provides important support for the development of modern industry. At present, continuous casting technology is widely used in the steel industry. The steel smelting and continuous casting system is generally composed of carbon composite functional refractories.

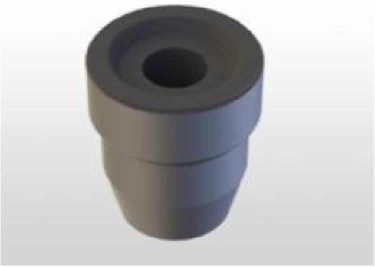

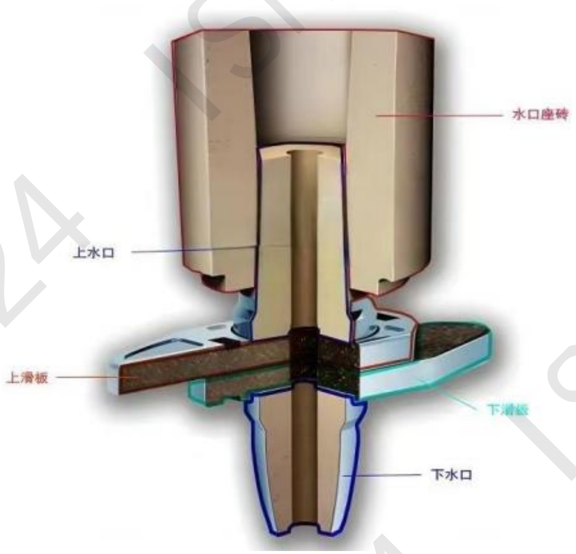

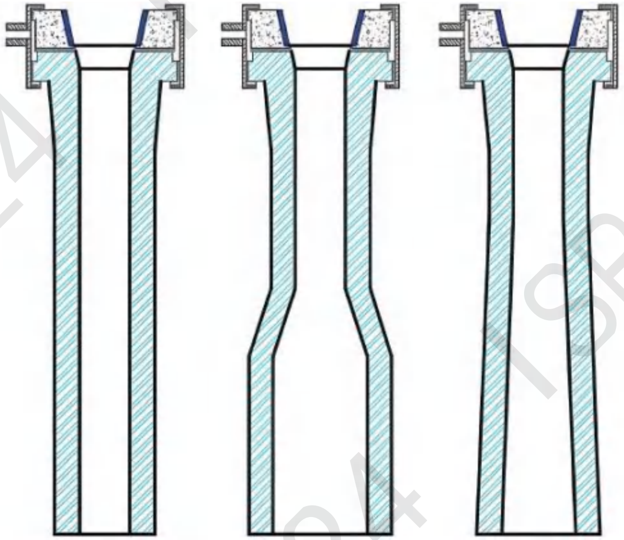

1. Background

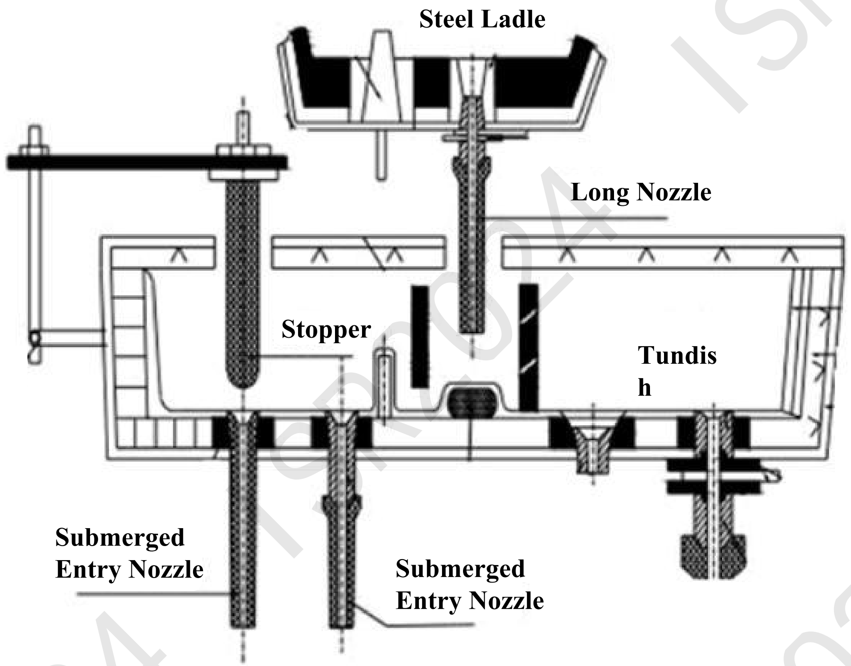

- Chemical attack (corrosion)
- Physical/mechanical wear (such as erosion/abrasion)
- Oxidation behavior
- Thermal shocks

Formation of micro-cracks inside the carbon composite refractory, which may fail suddenly in extreme cases.

1. Background

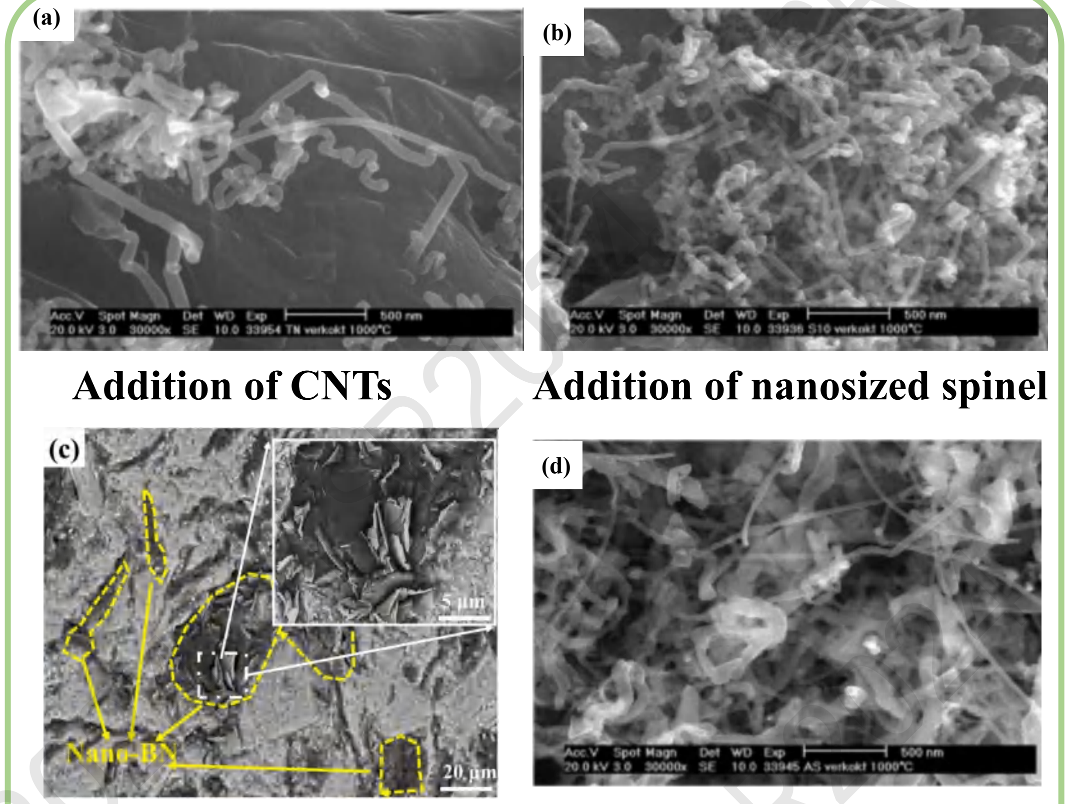

Addition of CNTs **Addition of nanosized spinel**

Addition of nano-BN **Addition of alumina sheets**

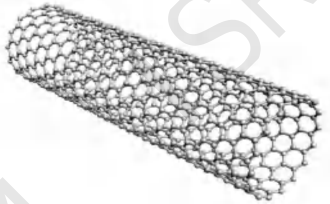

These nanoscale carbon sources and additions played a variety of roles.

- The promotion of **whisker growth**
- **Larger** surface area and **higher** reactivity

↓

- The improving the **performance** of Al_2O_3-C refractory
- The reduction **carbon content**

V. Roungos, C.G. Aneziris, Improved thermal shock performance of Al_2O_3-C refractories due to nanoscaled additives, Ceram. Int. 38 (2) (2012) 919–927.
Y.X. Luo, X. Wang, Z.L. Liu,et al. Enhanced oxidation resistance and thermal shock resistance of low-carbon Al_2O_3-C refractories with nano-BN: a synergistic of mullitization behavior, J. Alloys Compd. 25 (2024) 172937.

武汉科技大学
WUHAN UNIVERSITY OF SCIENCE AND TECHNOLOGY

1. Background

MAX phase is a new type of ternary layered compound with highly ordered structure.

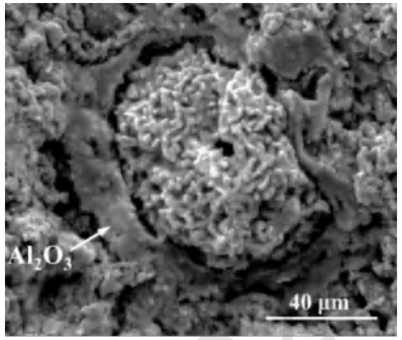

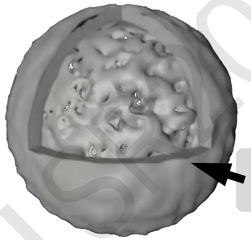

Al_2O_3dense shell

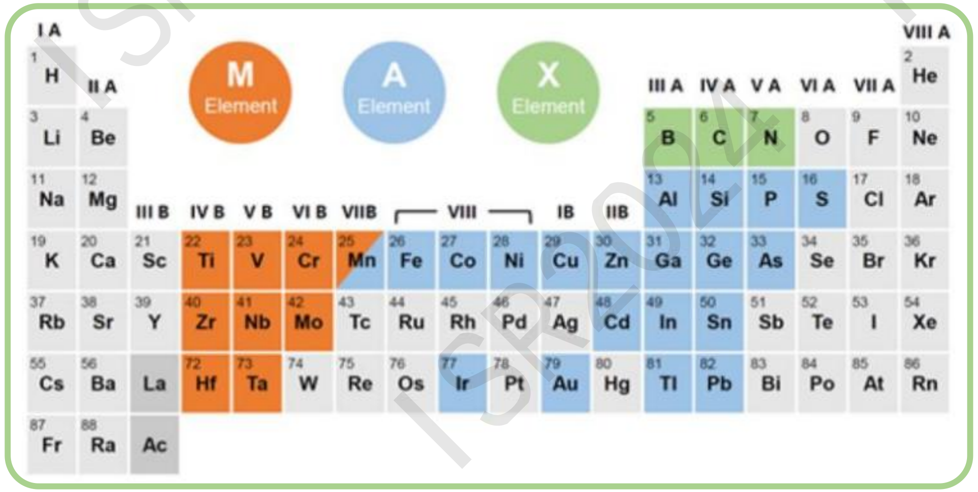

Crystal Structure of Cr_2AlC

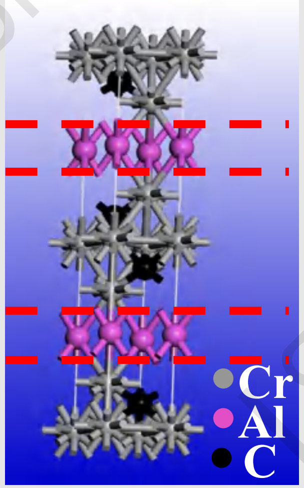

Excellent properties of metal and ceramic

- Good high temperature oxidation resistance
- Excellent thermal shock resistance and damage tolerance
- High elastic modulus and thermal conductivity

2. Experiment

The experimental formula of Al_2O_3-C refractory samples (wt.%)

Samples	AC-9	ACr-2.5	ACr-5
Sintered alumina aggregates (1-3mm, 0.088-1mm)	70	70	70
Sintered alumina powder (< 74µm)	19	19	19
Flake graphite (< 74µm)	9	6.5	4
Cr_2AlC (d_{50}=42.812µm)	0	2.5	5
Silicon powder (< 45µm)	2	2	2
Phenolic resin	+4	+4	+4

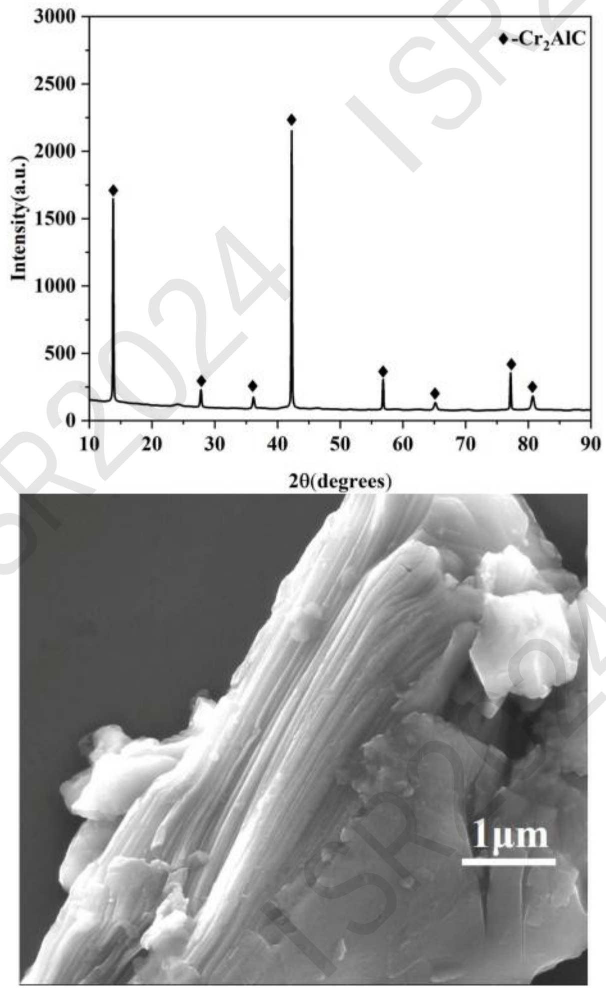

XRD pattern and Secondary electron image (SE) of the Cr_2AlC powders

Aggregates, Matrix(Cr_2AlC)

↓ mix

Mixture

↓ 150MPa

Samples

↓ 1100-1600°C

Sintered

↓

Test

3. Results

Mechanical properties

Mechanical characteristics of samples after heat treatment at different temperatures

		Linear change (%)	Bulk density (g/cm³)	Apparent porosity (%)	Modulus of Elasticity (GPa)	Rupture strength (MPa)
AC-9	220°C×24h	-	2.90±0.04	15.59±0.06	23.78±3.33	10.03±2.41
	1100°C×3h	0.07±0.08	2.88±0.05	16.86±0.99	16.58±3.20	5.72±1.52
	1400°C×3h	0.09±0.05	2.89±0.09	17.38±2.95	24.02±1.89	9.35±0.33
	1600°C×3h	0.06±0.05	2.85±0.04	19.78±0.14	24.43±0.23	10.27±0.61
ACr-2.5	220°C×24h	-	2.97±0.01	14.62±0.36	28.70±6.00	10.21±0.91
	1100°C×3h	0.05±0.02	2.97±0.01	16.47±0.59	15.89±1.53	4.96±0.71
	1400°C×3h	0.05±0.05	2.95±0.05	17.26±1.43	31.20±1.38	9.22±0.57
	1600°C×3h	0.28±0.06	2.91±0.04	19.88±0.89	24.43±1.47	6.38±0.72
ACr-5	220°C×24h	-	3.00±0.01	14.66±0.31	31.95±1.78	9.45±1.27
	1100°C×3h	0.03±0.02	3.00±0.01	17.46±0.13	20.47±1.99	5.18±0.48
	1400°C×3h	0.09±0.01	3.07±0.01	15.89±0.32	36.28±0.57	8.88±0.70
	1600°C×3h	0.56±0.15	2.89±0.07	20.85±1.93	26.94±2.94	6.37±0.88

- CMOR decreased at 1600°C
- The higher heat treatment temperature led to volume instability of materials structure which resulted in the decrease in the CMOR of samples

3. Results

Microstructures

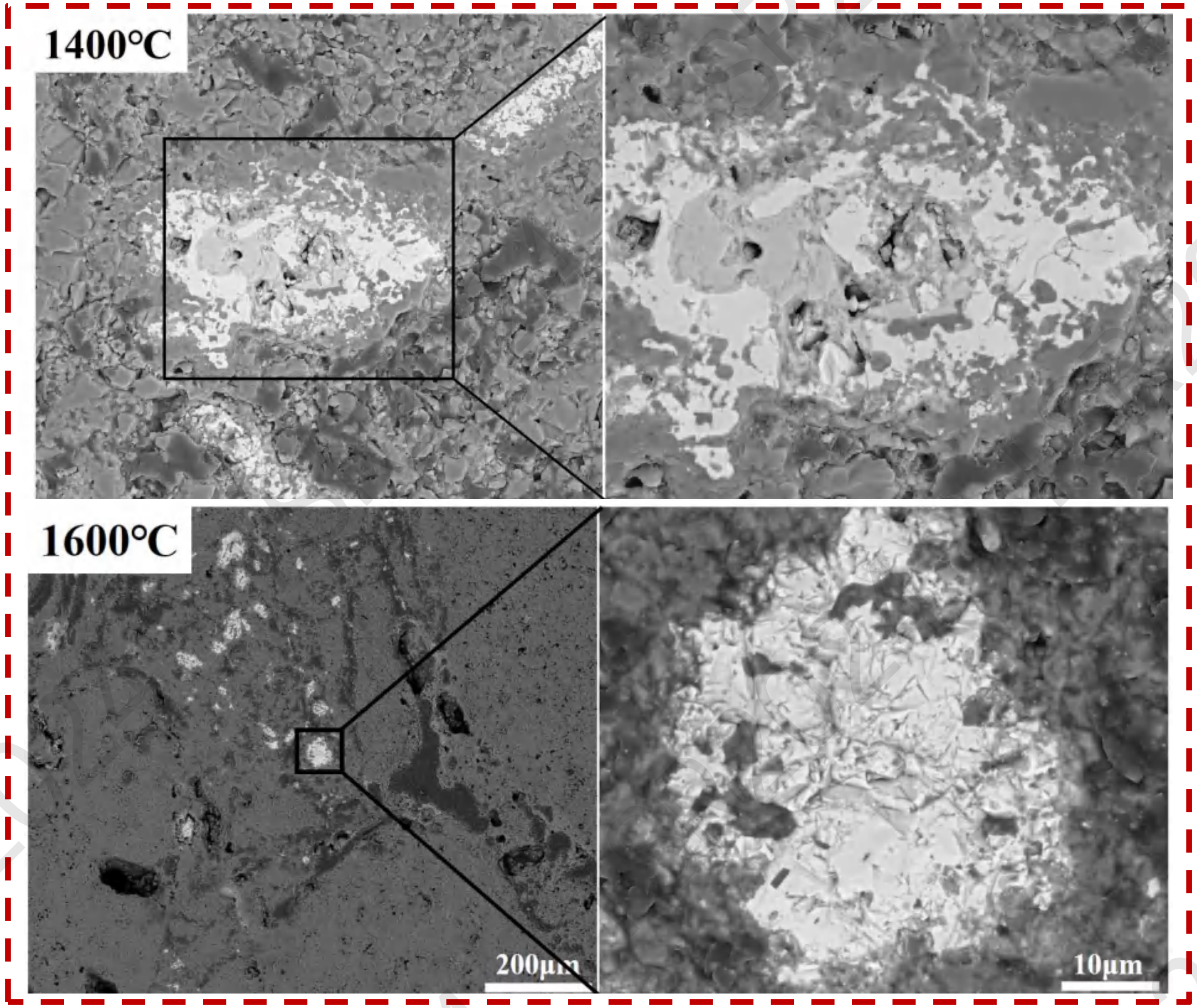

- Al element firstly migrated from the crystal site into the grain boundaries of Cr_2AlC grains, and then spread along grain boundaries to the outer layer, finally forming Al_2O_3 layer on the outer layer of Cr_2AlC particles.
- At 1600°C, the out-diffused and then oxidized aluminum was filled between the external Cr_2AlC particles, and little aluminum could be detected inside the particles.

3. Results

High temperature mechanical properties

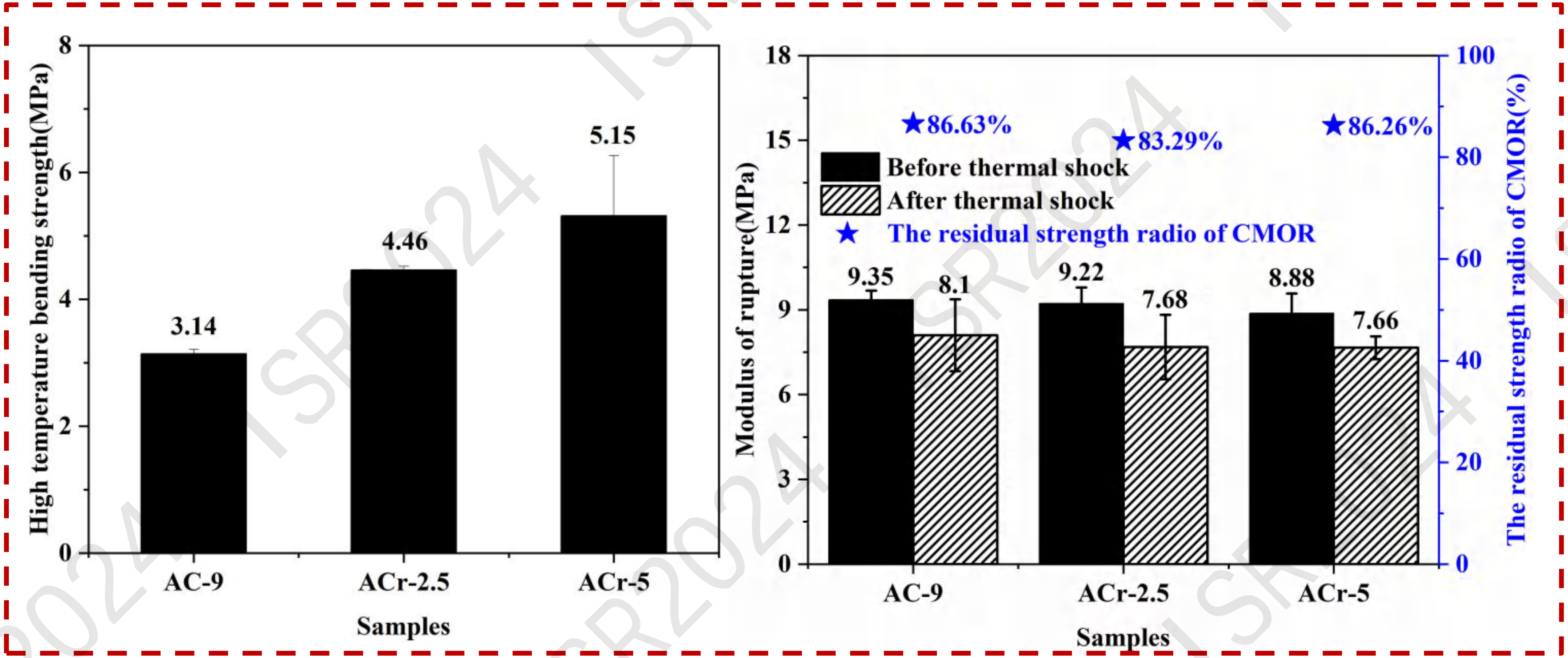

- The excellent thermal conductivity of Cr_2AlC.
- A dense coating with Al_2O_3 formed on the Cr_2AlC grain surface contributes to the bond strength of matrix.

3. Results

Corrosion resistance

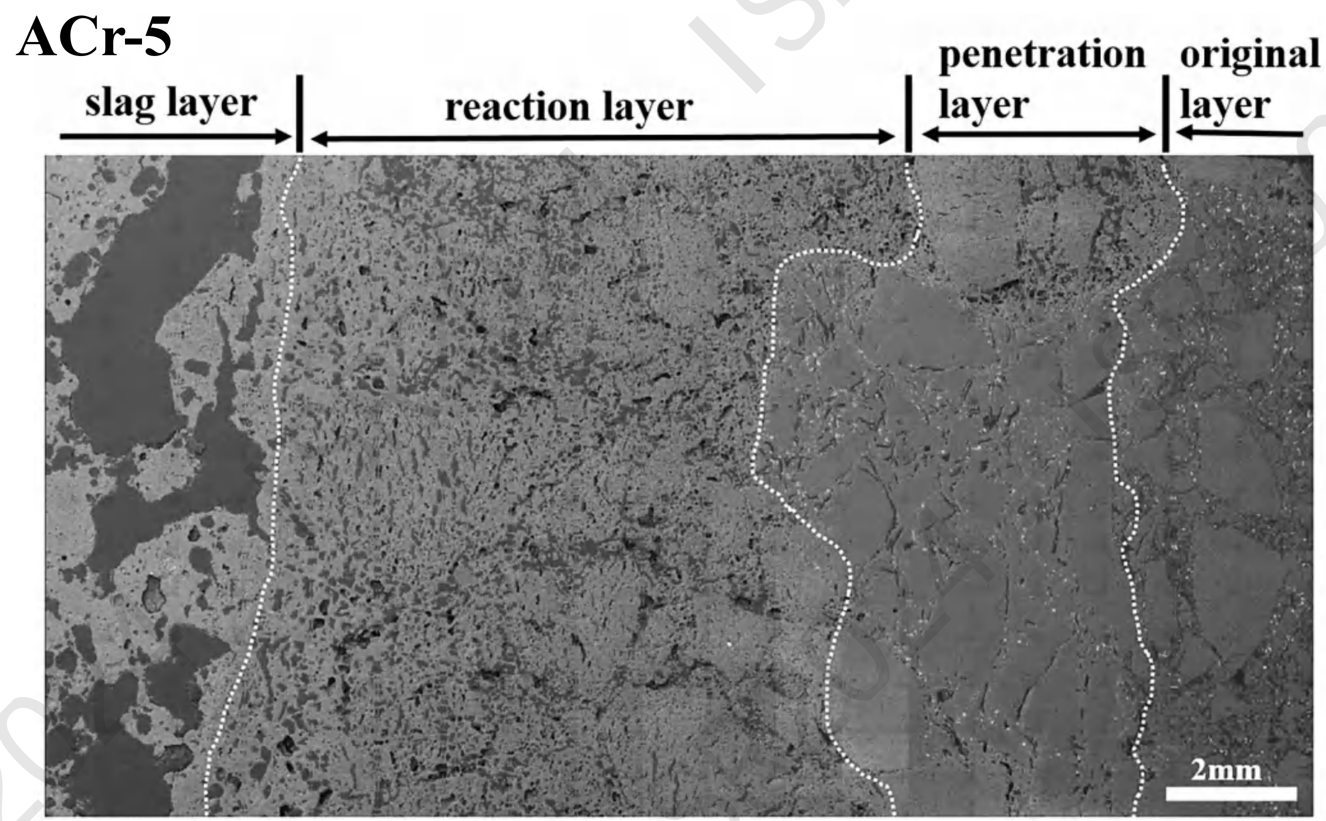

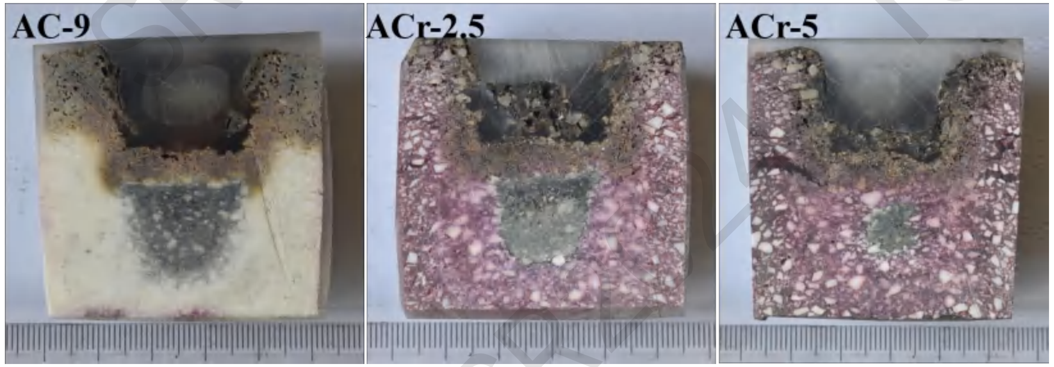

Cross-section of the samples with different Cr_2AlC contents after the corrosion test at 1600°C

The corroded microstructure consisted of slag layer with macro-pore structure, reaction layer, penetration layer and original layer.

3. Results

Corrosion resistance

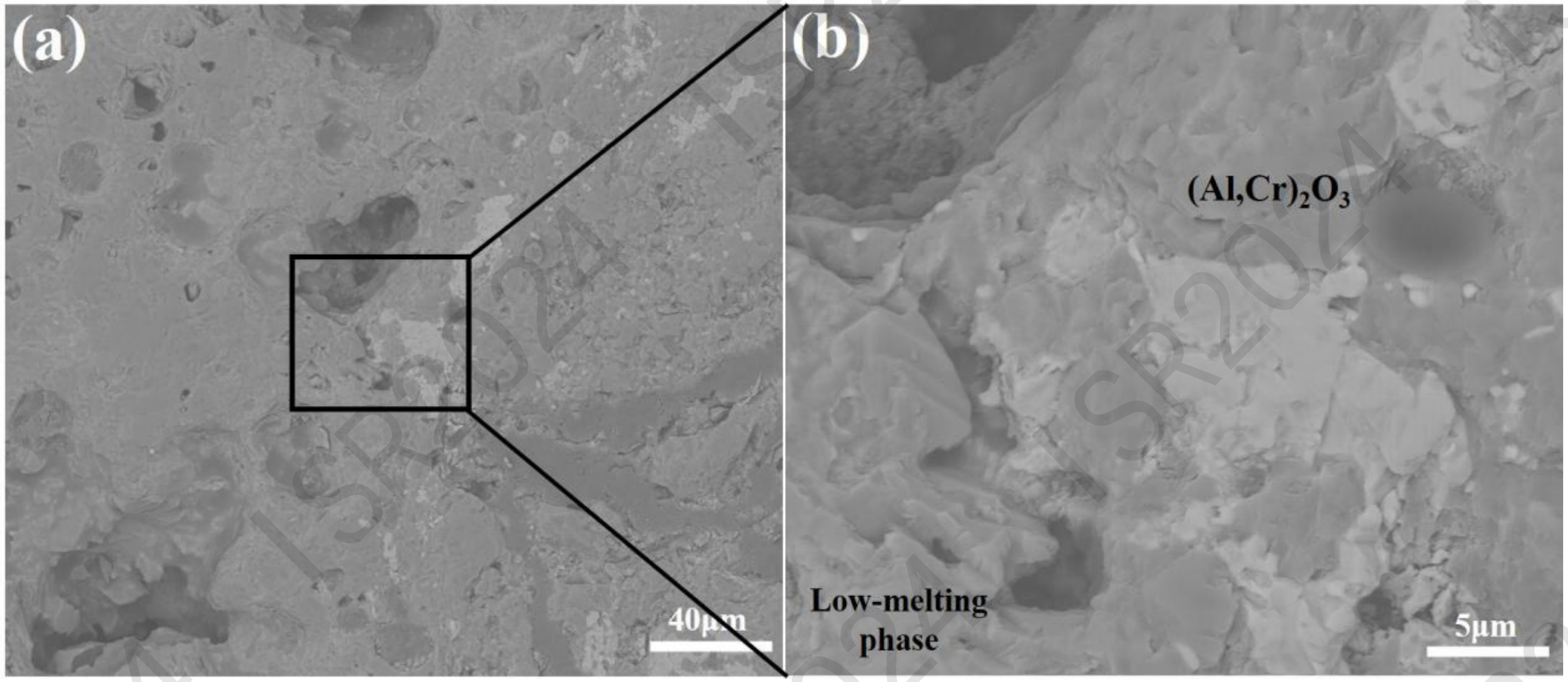

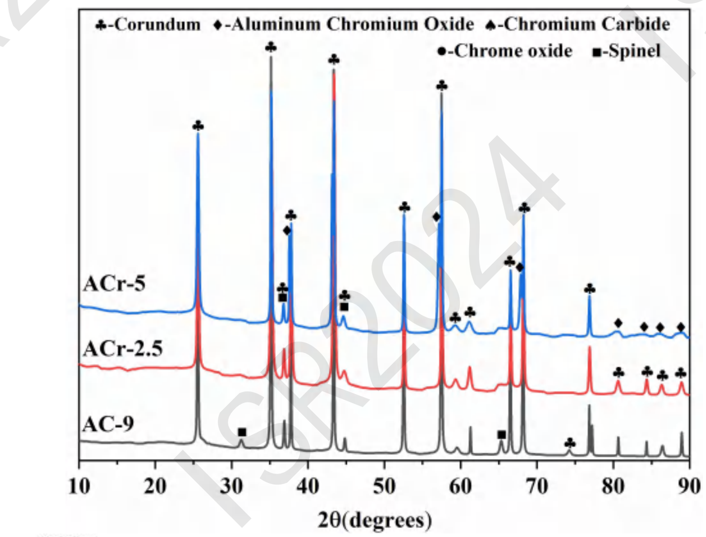

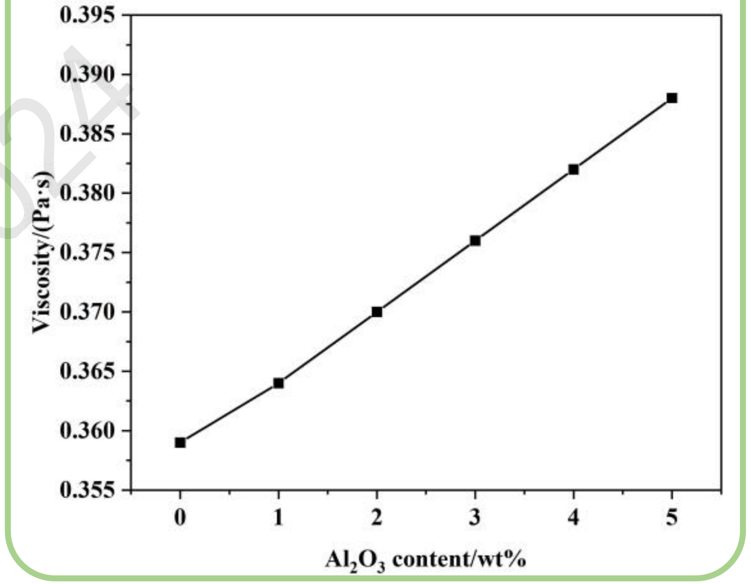

① $Cr_2AlC(s)+(3x/2)CO(g) \rightarrow Cr_2Al_{1-x}C(s)+(x/2)Al_2O_3(s)+(3x/2)C(s)$

② $Cr_xC_y(s)+ (3x/4+y/2)O_2(g) \rightarrow (x/2)Cr_2O_3(s)+yCO(g)$

③ $Cr_2O_3(s)+Al_2O_3(s) \rightarrow (Al, Cr)_2O_3(ss)$

4. Conclusions

- The HMOR of the Al_2O_3-C sample with 5wt% Cr_2AlC-adding after heat treatment at 1400℃ increased to **5.15 MPa** from **3.14 MPa**. Furthermore, the residual CMOR ratio did **not significantly decrease** when carbon content was reduced from 9 to 4wt%.
- The addition of Cr_2AlC in Al_2O_3-C refractories led to the **improvement in corrosion resistance**. The Al_2O_3 and Cr_3C_2 grains were first generated in the original Cr_2AlC grain boundaries at a lower temperature. Then the Al_2O_3 layer of Cr_2AlC surface suffered chemical attack from the penetrated slag, and reacted with Cr_2O_3 generated by further slag corrosion to form **$(Cr, Al)_2O_3$ solid solution**. The $(Cr, Al)_2O_3$ solid solution dissolved in the slag, **increasing the viscosity** of the slag and suppressing the further penetration of slag. The original Cr_2AlC gradually decomposed and finally dissolved into slag.

Thank you for your attention !

This work was project funded by the Key Project of the National Natural Science Foundation of China (Grant No. U21A2058), China Postdoctoral Science Foundation (2023M740971).